Supplementary materials

MATERIALS AND METHODS

Morphometric analysis

3D enamel thickness

To quantify the 3D enamel thickness, high-resolution micro-CT images of Bombrini, as well as 18 recent *Homo sapiens* (RHS) deciduous lower second incisors (Northern Italian Medieval and Renaissance specimens housed at the Department of Cultural Heritage, Ravenna, University of Bologna, Italy) were obtained with the Xalt micro-CT scanner *(32)* (Institute of Clinical Physiology, National Research Council, Pisa, Italy). All teeth were scanned at 50 kVp, 2 mm Al filtration, 960 views over 360°, 1.6 mAs/view. All the images were reconstructed using a modified Feldkamp-type cone beam Filtered Backprojection (FBP) algorithm *(33)* with embedded compensation of mechanical misalignments. The isotropic voxel size of 18.4 μm^3 on a 512x512x1200 volume dataset and then cropped to the tightest bounding box of each tooth. The micro-CT images were segmented in MeVisLab 2.4 (MeVis Medical Solutions AG, Bremen, Germany) using a global threshold calculated as the mid-value (in Hounsfield Units) between the dentin and enamel peaks in the image stack histogram. The segmented enamel cap and virtually filled dentin were then converted to meshes using the Winged-Edge Mesh (WEM) tool and exported in Standard Tessellation Language (STL) file format for subsequent analysis.

Additional comparative data for five Neandertals (Abri Suard, Amud 7, Kebara 1, La Ferrassie 8, Roc-de-Marsal 1) were obtained with a BIR SN001 microtomographic system (Max Planck Institute for Evolutionary Anthropology, Leipzig, Germany) using the following scan

parameters: 130 kV, 100 µA, with a brass filter of 0.25 mm (for Abri Suard and Roc de Marsal 1) and 0.50 mm (for Kebara 1 and Amud 7) thickness; 100 kV, 200 µA, with a brass filter of 0.25 mm for La Ferrassie 8. Volume data were reconstructed using isometric voxels ranging between 16.41 µm and 36.44 µm. The micro-CT images of the Neandertal sample were virtually segmented using a semiautomatic threshold-based approach in Avizo 7 (Visualization Sciences Group Inc.) to reconstruct 3D digital models of the teeth.

The digital models were then imported in Rapidform XOR2 (INUS Technology, Inc., Seoul, Korea). Following indications provided by Benazzi and colleagues *(16)*, the entire enamel cap was considered, while the coronal dentine was separated from the root dentine using a spline curve digitized along the cervical line. This curve was interpolated with a smooth surface to seal the bottom of the dentine core.

We measured the volume of the enamel cap (mm^3); the volume of the dentine core (which includes the volume of the coronal pulp - mm^3); the enamel-dentine junction (EDJ) surface (the interface between the enamel cap and the dentine core - mm^2). These measurements were used for the computation of both the 3D average enamel thickness (3D AET = volume of enamel divided by the EDJ surface; index in millimeters) and the 3D relative enamel thickness index (3D RET = the average enamel thickness index divided by the cubic root of dentine volume; scale free index) (Table S2). Standardized scores (Z-scores) of Bombrini crown BL diameters and RET index were computed to establish to which group means the value of Bombrini was closest to.

Digital simulations of tooth wear and mesial damaging

Since Bombrini is rather worn and the enamel is chipped off mesially, two RHS specimens (Guid_T39 and Sgvald_T59) were digitally worn down and mesially damaged simulating a condition comparable to Bombrini to evaluate whether the loss of enamel on the mesial side of the Bombrini tooth affects the computed AET and RET indices, and ultimately its taxonomic attribution. Since Ungar and colleagues *(34)* did not find any clear pattern of beveling with tooth wear in permanent lower incisors, we defined an objective procedure to digitally wear and damage the two RHS specimens that involves the following steps (Fig. S8): the best-fit plane through the points of the incisal surface (incisal plane) of Bombrini was computed (Fig. S8A); the crown of the two RHS specimens was superimposed to the crown of Bombrini using Iterative Closest Point, an algorithm that minimizes the distance between two point clouds by the least squares method *(35)* (Fig. S8B), and the portion of crown above the incisal plane was removed (Fig. S8C); for both RHS specimens, the portion of enamel in correspondence to the Bombrini's mesial damage was removed (Fig. S8C), whereas the underlying dentine was preserved (Fig. S8D), and the 3D enamel thickness was computed (Table S3).

Ancient DNA

DNA extraction and library preparation

A sample of 20mg was removed from the root of the tooth using a sterile dentistry drill. DNA was extracted as described *(36)* and eluted in 100µl of TE (10mM Tris-HCl, 1mM EDTA, pH 8.0). Three libraries (A4678, L9358 and A4679) were prepared using 5µl, 10µl and 15µl of DNA extract, respectively. Library L9358 was pre-treated with USER (New England Biolabs), a mixture of uracil DNA glycosylase (UDG) and endonuclease VIII, which removes uracil bases

from the interior of DNA molecules *(37, 38)*. In contrast, libraries A4678 and A4679 were not treated with USER, in order to maintain the complete C to T substitutions signal. All three libraries were created using a single-stranded DNA library preparation protocol *(39)*. The number of DNA molecules in each library was determined by digital droplet PCR (BioRad QX 200), using 1µl of a 4,000-fold dilution of libraries A4678 and A4679 and a 8,000 dilution of library L9358 as template for an EvaGreen (BioRad) assay with primers IS7 and IS8 *(40)*. Each library was tagged with a pair of unique indexes *(41)* and amplified using AccuPrime Pfx DNA polymerase (Life Technologies) *(42)*. Amplification products were purified using the MinElute PCR purification kit (Qiagen).

Mitochondrial capture and sequencing

0.6µg of library L9358 was enriched for human mtDNA once, as described *(43)*. Libraries A4678 and A4679 were enriched twice (using 1µg of library for the first round and 0.5µg for the second round) as described *(44)*, except that the hybridization and post-hybridization wash temperatures were 60°C and 55°C, respectively *(22)*. The enriched libraries were sequenced on Illumina's MiSeq platform using two paired-end runs (2x 76 cycles) with double-index configuration *(41)*.

Raw sequence processing and mapping

Base calling was performed using IBIS *(45)* for library L9358 and using Bustard (Illumina) for libraries A4678 and A4679. Only sequences which perfectly matched the expected index combinations were retained. Adapter sequences were trimmed, and forward and reverse reads were merged into a single sequence *(46)*. Merged sequences were aligned to the revised

Cambridge Reference Sequence (NC_012920), using BWA *(47)* with the parameters "-n 0.01 -o 2 -l 16500", with seeding turned off and allowing for more mismatches and gaps than default parameters *(38)*. PCR duplicates were removed by calling a consensus from sequences with identical alignment start and end coordinates.

Phylogenetic inferences

Two sets of diagnostic positions were generated. The first is composed of 63 positions at which modern humans (n=311) *(23)* differ from all ten Neandertals for which complete mtDNA genomes have been sequenced. The second set is composed of 17 positions at which modern human mitochondrial genomes (n=311) differ from the Neandertal (n=10), Denisovan (n=3) and chimpanzee (*Pan troglodytes*) (n=1) genomes. Each analysis was carried out twice, once using all mapped sequences at least 35bp in length and once using only sequences with a C to T difference to the reference genome at the 5' and/or 3' terminal position.

Radiocarbon chronology

Samples selection and Method

In order to investigate the chronology of Palaeolithic sites, sample selection is the first aspect that should be considered. Bones with anthropogenic marks are the best samples to attest human presence at a site. However, this type of selection process can contribute to affect the preservation of collagen *(3)*. In addition, the number of samples taken for radiocarbon dating is the second most important factor to be considered, in order to constrain the chronological events at the site.

At Riparo Bombrini, 32 samples were selected for radiocarbon dating; 29 animal bones (with and without anthropogenic marks) and three charcoal samples.

All 29 bone samples were pretreated at the Department of Human Evolution, Max Planck Institute for Evolutionary Anthropology (MPI-EVA), Leipzig, Germany, using the method described in Talamo and Richards *(48)*. The outer surface of the bone samples are first cleaned by a shot blaster and then 500mg of bone powder is taken. The samples are then decalcified in 0.5M HCl at room temperature until no CO_2 effervescence is observed, usually for about 4 hours. 0.1M NaOH is added for 30 minutes to remove humics. The NaOH step is followed by a final 0.5M HCl step for 15 minutes. The resulting solid is gelatinized following Longin *(49)* at pH3 in a heater block at 75°C for 20h. The gelatine is then filtered in an Eeze-Filter™ (Elkay Laboratory Products (UK) Ltd.) to remove small (<80 μm) particles. The gelatine is then ultrafiltered with Sartorius "Vivaspin Turbo" 30 KDa ultrafilters *(50)*. Prior to use the filter is cleaned to remove carbon containing humectants *(51)*. The samples are lyophilized for 48 hours.

To verify the state of preservation of the collagen, the C:N ratio, %C, %N, collagen yield and $\delta^{13}C$ and $\delta^{15}N$ values must be evaluated. The C:N ratio should be between 2.9 and 3.6 and the collagen yield not less than 0.5% of weight *(52, 53)*. Stable isotopic analyses were undertaken at MPI-EVA, Leipzig (Lab Code S-EVA), using a Thermo Finnigan Flash EA coupled to a Delta V isotope ratio mass spectrometer.

The 13 bones that met the collagen quality criteria (Table S6) were sent to the Klaus-Tschira-AMS facility of the Curt-Engelhorn Centre in Mannheim, Germany (Lab Code MAMS), where

they were graphitized and dated *(54)*. The three charcoal samples were sent directly to the Mannheim AMS laboratory, where they were pretreated with the ABOX method.

Chronological work at Riparo Bombrini

It should be pointed out that the G. Vicino excavation of 1976 was carried out through partially cemented sediments (as mentioned above in "*The discovery of the tooth"* paragraph), which were not affected by stratigraphic disturbances. On the other hand, some areas excavated in 2002-2005, located NW and SE of the 1976 trench, are probably problematic from a stratigraphic point of view. Here, soil forming processes affected the sequence in squares D1-F1 of the NW sector, outside the probable dripline of the former rock-shelter, and, consequently, the stratigraphy was difficult to read during fieldwork. However, the diagnostic lithic artefacts in these deposits were exclusively Protoaurignacian, suggesting that no major reworking occurred.

Pedogenesis was less developed within the inner part of the shelter, but disturbance may have been produced by the dumping of a large heap of waste exactly on top of the Bombrini deposits during the 19th century railway works or World War II destructions.

However, it must be stressed that the site yielded only Protoaurignacian artefacts, and that no evidence of more recent cultural phases was identified in the shelter. If more recent levels existed, they were destroyed by the construction of the railway in 1870; in fact, very rare reworked Gravettian-Epigravettian tools were found only in the spoil heap of the railway construction works.

For these reasons we kept the two areas of excavation separate when we performed the Bayesian analysis. The radiocarbon results of Riparo Bombrini are listed in Table S6.

All dates were corrected for a residual preparation background estimated from pretreated ^{14}C free bone samples, kindly provided by the MAMS and pretreated in the same way as the archaeological samples.

All the samples were calibrated using IntCal13 *(24)* in the OxCal 4.2 program *(29)* (Fig. 2 and Fig. S9, Table S9). The t-type outlier analysis was performed to detect problematic samples, with prior probabilities set at 0.05. The results were linked with the (NGRIP) $\delta^{18}O$ climate record (*55*, *56*).

Supplementary online text

RIPARO BOMBRINI

Description of the site and history of the excavations

Riparo Bombrini is situated in an important archaeological area of shelters and caves known as Balzi Rossi (literally 'Red Rocks'), an impressive Jurassic dolomitic limestone cliff located on the Italian-French state border and facing the present-day seashore (Fig. S1). The name of the locality derives from the iron-rich minerals included in the limestone walls. The complex includes several caves and shelters, the most famous of which are Grotta dei Fanciulli, Riparo Lorenzi, Grotta di Florestano, Grotta del Caviglione, Barma Grande, Grotta del Bauso da Ture (now destroyed), Grotta del Principe, Grotta Costantini, Riparo Mochi and Riparo Bombrini (Fig. S2). Florestano I, Prince of Monaco, carried out the first archaeological research at Balzi Rossi in 1846-57. More recently, between 1928 and 1961, regular excavations were carried out by Alberto Carlo Blanc, Luigi Cardini, Paolo Graziosi and Aldobrandino Mochi, on behalf of the Italian Institute of Human Palaeontology *(57)*.

The richest series of Palaeolithic Venuses ever found in one place in Western Europe was discovered between 1883 and 1895 by Louis Alexandre Jullien at Barma Grande *(58)*; more recently, Upper Palaeolithic engravings and an incision representing a horse on the wall of Caviglione were also discovered *(59-61)*. Unfortunately, most of the caves were excavated by the first pioneers and explorers of the nineteenth century, and little or no stratigraphic information from these earlier excavations is available.

More recently, research was resumed: by the Musée d'Anthropologie Préhistorique de Monaco at Grotta del Principe, where a fossil fragment ascribed to *Homo heidelbergensis* was recovered in an Early Palaeolithic layer *(62)*; by Giuseppe Vicino at the site of the Ex-Casinò *(63, 64)*; by Mauro Cremaschi at the site of the Ex-Birreria *(65)* and by Amilcare Bietti and other scholars at Riparo Mochi *(66-72)*.

Balzi Rossi is one of the most important prehistoric sites in Europe, because it preserves stratigraphic sequences that include layers with traces of Neandertal and anatomically modern human occupation. Here, the arrival of modern humans was much earlier than at other sites in Italy, as indicated by the radiocarbon dates for the Riparo Mochi sequence *(70)*. Moreover, several complete Gravettian burials have long been the focus of extensive anthropological research at international level *(73-75)*.

Riparo Bombrini is situated in a narrow area between the railway line connecting Genoa to Nice and an old storage-tank, not far from Grotta del Caviglione, where the engraving of the horse and the famous grave of the “Homme de Menton” (actually a woman) were found. The prehistoric sequence of this shelter was discovered by Émile Rivière during the second half of the XIX century *(74)*, but was excavated for the first time in 1938 by Luigi Cardini *(77)*. His small trench unearthed layers that can be ascribed to the Protoaurignacian. Cardini also found hearths, bones and abundant lithic artefacts, among which several characteristic Dufour bladelets. The shelter was explored again in 1976 by Giuseppe Vicino, during works for the construction of a pedestrian bridge that crosses over the railway and leads to the caves *(78)*. This new excavation explored an area 6 m^2 wide and about one metre deep. The human tooth analysed in this paper

was discovered during these excavations *(79)*. Vicino unearthed a stratigraphic sequence formed by a thick layer with Protoaurignacian artefacts, overlying layers with Mousterian industries. Between 2002 and 2005, new archaeological excavations were carried out, with the goal of better understanding the Late Mousterian to Protoaurignacian transition. The rockshelter was excavated jointly by the Archaeological Superintendency of Liguria, the University of Pisa (Italy) and Duke University (North Carolina, USA), with the help of the Museo di Archeologia Ligure (Genova Pegli, Italy) and of the Istituto Internazionale di Studi Liguri (Bordighera, Italy). These last excavations were conducted next to the trench opened by G. Vicino, mainly focusing on Protoaurignacian layers, but also exploring Mousterian levels in a deep sondage *(72, 80-85)*.

Stratigraphy

The stratigraphy presented here refers to the 1976 and 2002-2005 excavations (Fig. S3). The site was explored over an area of about 15 m^2. A trench approximately 10 m long, almost perpendicular to the wall of the former shelter, was excavated into the archaeological deposit to a maximum depth of 130 cm *(67, 81-83)*.

Some minor differences in the description of the stratigraphy occurred during the two campaigns. The sequence was divided into four artificial spits by G. Vicino in 1976, who identified two cultural units: the lower one (Upper and Lower level IV) containing Mousterian material culture, the upper one (level III-I) containing Upper Palaeolithic artefacts. During the 2002-2005 excavations, the G. Vicino units were confirmed, but labelled differently. A description of the units identified during the latest field-work campaigns (2002-2005) and their correspondence

with the levels defined by G. Vicino (1976 excavation) is reported here from the lowermost (oldest) to the uppermost (most recent):

- M7-M1: levels with abundant Mousterian industry, corresponding to “Lower level IV” of the 1976 excavation.
- MS2-MS1: levels with scanty evidence of Mousterian industry, corresponding to “Upper level IV” of the 1976 excavation.
- A3: it is the infill of a narrow channel with sub-cylindrical bottom, running along the wall of the shelter; it included calcareous rubble mixed with very few Protoaurignacian artefacts; charcoal useful for dating was absent. This level has no correspondence with the deposits explored by the G. Vicino excavation.
- A2: level with very abundant Protoaurignacian artefacts; it corresponds to “level III” of the 1976 excavation.
- A1: level with abundant Protoaurignacian artefacts, corresponding to “level II” of the 1976 excavation.
- Level I was identified only during the 1976 excavation and yielded several *Mytilus* sp. shells, probably representing food refuse, but diagnostic artefacts were not present *(78)*.

Within the sequence, there is a sharp change between the lithostratigraphic units including Mousterian evidence and those with Protoaurignacian industry. The latest Mousterian is included within units MS2 and MS1, characterised by large breakdown blocks suggesting a cold climate phase. The transition between these units and those above, containing Protoaurignacian artefacts, is marked by a clear discontinuity, which shapes the top of unit MS1 and testifies either a stop of sedimentation or an erosive phase. Levels A2 and A1 (respectively level III and II in G. Vicino

excavation) are two artificial partitions of a single lithologic unit consisting of a yellowish silty-clay layer - probably a more or less altered loess - that includes abundant Protoaurignacian industry. Two superimposed hearths were found near the bottom wall of the shelter, respectively in levels A2 and A1; the lower one was situated inside a circular depression ("*en cuvette*") *(84)*.

The 1976 and 2002-2005 excavations yielded a very large quantity of knapped flint artefacts referable to the Protoaurignacian. Dufour bladelets are well represented, while formal tools and cores are scarce. Local raw material was mostly used, but exotic flint was also imported from France (Vaucluse, Estérel massif, various Provence outcrops) *(81, 84)*. Red radiolarite and *Scaglia rossa* flint are also present; the former comes from eastern Liguria and from the Parma area (Monte Lama-Catellaccio-Pràrbera), the latter from the Marche region, some 350 km away, on the Adriatic side of the Italian peninsula *(81, 86, 87)*.

Bone artefacts and personal ornaments such as perforated shells, steatite artefacts, engraved belemnites, worked bones, red ochre are also relatively common.

Fauna is well documented. It mainly comprises numerous small and often burnt bone fragments. Roe deer (*Capreolus capreolus*), chamois (*Rupicapra rupicapra*), and ibex (*Capra ibex*) are particularly abundant, indicating a relatively cold climate *(81)*.

The discovery context of the human tooth

The tooth was collected in 1976 by G. Vicino, while breaking a chunk of cemented sediment. It came from square B1, spit III-4, about 6 meters away from the shelter wall (Fig. S3, S4). It was lying about 70 cm below the surface, very close to a Dufour bladelet (Fig. S5), and it was

covered by layer I, layer II and by the upper spits of layer III *(82, 83)*. As mentioned above, the level I is not diagnostic and the levels III and II include Protoaurignacian artefacts.

The deposit excavated in 1976 was thicker than in the neighbouring areas and partially cemented. The uppermost part of the deposit, corresponding to “layer I”, formed a bulge in squares A1-B1. The 1976 field journal reports the following information on square B1: *"the central-front [NE] part of the square is occupied by a prominence, slightly to strongly cemented. […] This thicker part was designated as layer I because its characteristics are very different from the top of square C1"* (“la parte centrale anteriore del quadrato è occupata da una serie in rialzo, mediamente o fort. (fortemente) concrezionata. […] Questo spessore maggiore è stato indicato come strato I in quanto presenta caratteristiche molto diverse dalla superficie di C1”) (G. Vicino, unpublished excavation report). These statements are also confirmed by Vicino *(82)*, showing that later cementation by percolating CaCO3 preserved the sediment from reworking.

GROTTA DI FUMANE

Description of the site and history of the excavations

Grotta di Fumane (45.6° Lat, 10.9° Long) is situated in the Monti Lessini, a mountain group of the Veneto Alpine fringe; it lies at the base of a rock cliff at 350 m a.s.l., on the left of a small tributary stream flowing eastwards into the main Fumane Valley (Fig. S1). This important site was already known in the 19th century, and the first explorations were carried out by the Natural History Museum of Verona in 1964 and 1982, at the bottom of a sequence exposed by a road cut in 1950. New investigations started in 1988 *(15)*, under the patronage of the Superintendency for the Archeological Heritage of Veneto, and exposed a sequence of Palaeolithic occupation levels. Excavations are carried out yearly, since then, by the University of Ferrara.

The cave is part of a fossil karst complex excavated in the Ooliti di San Vigilio carbonatic sandstone (upper Lias), which is extensively dolomitized in the valley where the cave opens. The cave conjoins with other tunnels, and was completely obstructed by sediments and by the collapse of the external part of the roof. A sheltered area of almost 60 m^2 was unearthed after these rockfall deposits were removed, between 1990 and 1996, and extensive excavations were undertaken, with the aim of investigating evidence of the final Mousterian and Aurignacian occupations.

Stratigraphy

The whole cave complex preserves a sedimentary sequence 12 meters thick, divided from the bottom upwards into four macro-units labeled S, BR, A and D, which record the main climatic events that occurred between the Early and the Middle Würm *(88, 89)* (Fig. S6). Macro-unit A

includes several horizontally layered beds from A13 to A1. Sediments from the Mousterian to the Aurignacian levels are mostly comprised of frost-shattered slabs with variable amounts of sand and aeolian dust, the former being prevalent in the western zone, the latter increasing progressively from the entrance to outside of the cave. Lithics, faunal remains, hearths and other structures embedding fine levels are densely scattered on the ground, particularly in units A11, A10, A9, A6-A5 (Mousterian) and A2, A1 (Protoaurignacian); conversely, less dense groups of these features, or isolated combustion structures and lithic workshops are preserved in units A5 (final Mousterian), A4, A3 (Uluzzian), D3, D1 (Aurignacian). The Late Mousterian and Uluzzian sequence and their cultural remains are described in several articles *(90-97)*. Layer A2 was excavated at different times since 1988 and over variable extensions in the area of the cave entrance. The most extensive investigations were carried out from 1988 to 2005. The archaeological material was either directly excavated using a 33 x 33 cm grid, or recovered from wet sieving. Macro-unit D tops the sequence and occludes the cavities, outlining the present-day slope morphology. Its origin is mainly due to several rockfall events, followed by stabilization and affected by cryoturbation. Human presence, was intense in the lower Aurignacian units (D3d, D3b and D3a), and became sporadic in the middle level D1d, in which some Gravettian artefacts were found *(98)*.

The discovery context of the human tooth

The tooth was found in square 91b (Fig. S7), well embedded in the sediment of unit A2. Layer A2 is a clearly discernible layer (preserved with variable thickness all over the cave entrance, from a few centimetres to 10 cm in thickness), due to its dark colour and its high charcoal, bone and stone implement density, and occurrence of dwelling structures (i.e. hearths, post-holes,

waste dump areas). The stone implements are blades, retouched bladelets and Dufour bladelets. Other finds include bone and antler tools, painted stones (possibly parietal art), accumulations of ochre and over 800 mollusc shells *(99-103)*. A revised chronology of the Mid-Upper Palaeolithic sequence at the Grotta di Fumane *(10)* has shown that the start and the end of level A2 date respectively to 41,900-40,200 cal BP and 40,300-39,400 cal BP at the largest confidence interval.

THE HUMAN FOSSIL REMAINS

Morphological description

Bombrini

Lower left lateral deciduous incisor (Ldi_2) with partially-preserved crown and cervical quarter of the root (Fig. 1). The enamel is chipped off mesially, and there is a deep crack on the lingual side of the crown, which emanates from a second crack that runs mesio-distally. The incisal surface is worn, exposing a large area of dentine equivalent to wear stage 4 *(19)*. The crown appears asymmetrical in occlusal view, owing to a pronounced mesio-distal convexity that includes about two thirds of the labial and lingual surfaces, and to a slight concavity of the distal third. On the lingual side, there is a moderate lingual cervical eminence, but no tubercle-like structure; above this, the surface is concave, and shows faint mesial and distal marginal ridges, which reach the cervical eminence. An interproximal wear facet can be observed on the distal side, but not on the mesial one, and was probably removed by the mesial damage.

The preserved root stump is more elongated labially (4.1 mm) than lingually (1.6 mm), and appears to be resorptive, confirming an age of approximately 6 years on the basis of recent human standards *(104, 105)*. There is no evidence of either caries or enamel hypoplasia.

The tooth crown has a MD diameter of 4.3 mm (minimum estimation due to wear and mesial damage) and a BL diameter of 4.6 mm. At the cervix, the MD diameter is 3.2 mm and BL diameter is 4.4 mm. The computed Z-score for BL crown diameters shows that Bombrini is closer to the Upper Paleolithic *H. sapiens* mean (Table S1).

Fumane 2

Fumane 2 is an upper right lateral deciduous incisor (Rdi^2) with well-preserved crown and less than half of the root preserved (Fig. 1). A large fissure crosses the tooth mesio-distally, with a second one emanating from it towards the labial side. The incisal surface shows strong oblique wear (wear stage 6 according to ref. *(19)* from mesio-labial to disto-lingual. This wear removed nearly all the lingual enamel, except where it covers a lingual cervical prominence (not a tubercle-like structure). The labial border of the incisal edge is chipped, probably because of para-masticatory activities. The crown appears symmetrical in occlusal view, and the preserved part of the labial surface is evenly and weakly convex mesio-distally. An interproximal wear facet can be observed on the distal side, but not on the mesial one, probably removed by wear.
The short segment of the root, longer labially (6.1 mm) than lingually (0.8 mm), looks resorptive, indicating an age of ~6/7 years on the basis of recent human standards *(104, 105)*.

The tooth crown has a MD diameter of 5.9 mm (minimum estimation due to wear) and a BL diameter of 5.5 mm (Table S1). At the cervix, MD is 4.2 mm and BL is 4.9 mm. The computed Z-score for BL crown diameters shows that Fumane 2 is closer to the Neandertal mean (Table S1).

3D enamel thickness

The values of the components of 3D enamel thickness computed for Bombrini and the comparative sample (Neandertals and recent *H. sapiens*) are summarized in Table 1 and reported in detail in Table S2. For each tooth, the wear stage was evaluated following ref. *(19)*.

When two recent *H. sapiens* specimens are digitally worn down to the level of the Bombrini specimen, the AET index decreases of 0.04 mm and the RET index decreases of about 1 point, because tooth wear affects more the enamel volume than the dentine volume (Table S3). In addition, our results indicate that both AET and RET values remain quite stable when the artificially worn teeth are digitally damaged on the mesial side to simulate the condition observed in the Bombrini incisor, confirming both the reliability of the indices computed for Bombrini and that the original RET index (the index of the hypothetical unworn Bombrini incisor) should have been at least 1 point larger.

Ancient DNA

General characteristics of the libraries

The number of DNA molecules in each library, as quantified by digital droplet PCR, ranged between $3.8x10^9$ and $1.7x10^{10}$ (Table S4), and were higher than extraction and library preparation negative controls in the experiments (not shown), consistent with a successful library preparation (39). Following sequencing on a MiSeq (Illumina), the libraries yielded between 1.2 and 3.2 million reads (Table S4). Each unique sequence was seen on average 6.2, 19.7 and 27.6 times for L9358, A4679 and A4678, respectively (Table S4), indicating that deeper sequencing would not substantially increase the yield of mitochondrial sequences. After discarding all sequences shorter than 35bp, 1.9%, 4.4% and 6.0% of sequences (from libraries L9358, A4678 and A4679, respectively) could be aligned with a mapping quality score >30 to the revised Cambridge Reference Sequence (Table S4).

Nucleotide substitutions

All three libraries showed similar frequencies of cytosine (C) to thymine (T) substitutions at the 3' ends of sequences (14-17%). In contrast, the C to T substitution frequency on the 5' end in library L9358 was lower than that in the other libraries (Table S5). This difference can be explained by the pre-treatment of L9358 with *E. coli* UDG, which removes uracils more efficiently at the 5' than at the 3' end of molecules (38). In libraries A4678 and A4679, when filtering for sequences carrying a C to T change on one of their ends, the frequency of C to T substitutions on the other end increased (Table S5). This suggests that the sequences derive from a mixture of endogenous ancient DNA, which is affected by cytosine deamination, and present-day human contamination, which is not affected or affected to a much lesser extent (22). Library L9358 did not yield a sufficient number of sequences for this analysis, as apparent from the wide confidence intervals (Table S5).

Radiocarbon dating

Vicino 1976 excavation: Results and Discussion

Five samples from the G. Vicino excavation, from layer III to layer I, were dated. The radiocarbon results of the Protoaurignacian level (III and II) range from 33,980±160 to 29,950±260 ^{14}C BP. The bone sampled for level I, which is associated with Upper Palaeolithic material culture (albeit not diagnostic of the Protoaurignacian), dates to 29,660±250 ^{14}C BP. In this case, to better constrain the chronology of the G. Vicino excavation, the recently published dates on shells from the Mousterian deposit (level IV Table S7) *(4)* were included in the Bayesian model. Moreover, previous radiocarbon dates for Grotta di Fumane (Table S8) *(10)* were included in the OxCal 4.2 model, recalibrated with IntCal13, as a separate plot.

The overall Agreement index is 70.5% well above the minimal acceptable level of 60%. No outliers were detected when the t-type outlier analysis was performed, thus confirming the integrity of the sequence and the reliability of the chronology. The start calibrated boundary for the Mousterian level (level IV) ranges between 44,840 and 43,160 cal BP. The transition between the Mousterian level IV and the Protoaurignacian level II ranges between 40,710 and 34,190 cal BP. The age of the tooth from Bombrini, found in the level III, ranges between 40,710 and 35,640 cal BP in the model created by OxCal. However, given the two determinations for level III (MAMS-21663; ^{14}C Age 32,920±140 and MAMS-21662; ^{14}C Age 33,980±160), we believe that the tooth dates more likely to the unmodelled calibrated range from 38,670 to 36,560 cal BP. The Upper Palaeolithic part (level I) is calculated between 33,710 to 32,660 cal BP.

Excavation 2002-2005: Results and Discussion

The chronology of the deposits excavated in 2002-2005 is more complicated to establish (Fig. S9, Table S9). In this case, the outlier analysis detected three outliers (ca. 100%) in level A2: sample MAMS-21353 was identified as a 100% outlier, given its very young age. The Agreement index for the sequence is below the minimal acceptable level of 60% (A_overall 18.1%). These parameters already indicate disturbance in the more recently excavated area, as confirmed by the micromorphological evidence for mixing in the stratigraphy described above.

It is, therefore, difficult to state the true upper boundary of the Protoaurignacian for this part of the Riparo Bombrini deposits, due to the possible later disturbance produced by the Gravettian occupation. There is no clear evidence of diagnostic Gravettian assemblages in these layers, although some knapping by-products could be Gravettian. For this reason, we prefer to provide

only the lower boundary for this excavation area, which is comprised between 40,820 and 38,380 cal BP at 68.2% of confidence and 42,280 and 37,630 at 95.4%. These results are in agreement with the dates produced on organic remains from the G. Vicino excavation of 1976.

Fig. S1. Geographical distributions of the Protoaurignacian. The human remains associated with the Protoaurignacian, and considered in this study, were unearthed from Riparo Bombrini (Ventimiglia, Italy) and Grotta di Fumane (Western Lessini Mountains, Italy).

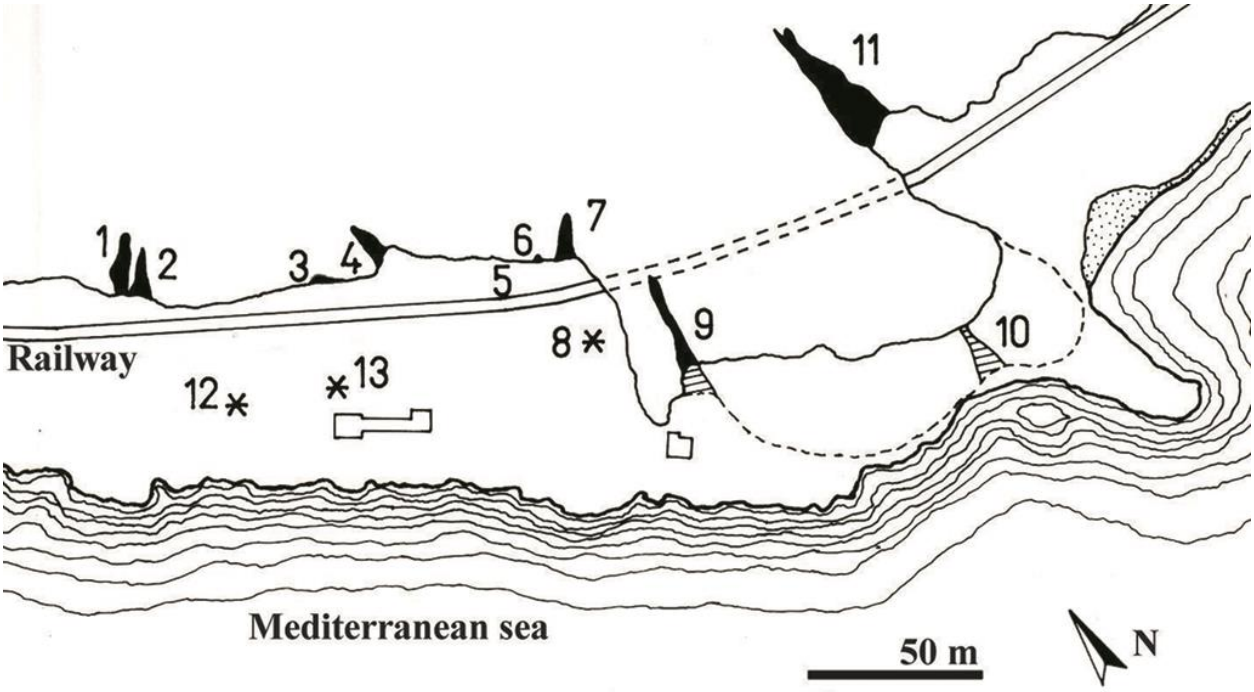

Fig. S2. The archaeological area of Balzi Rossi. Location of the sites: 1: Grotta Costantini; 2: Grotta dei Fanciulli; 3: Riparo Lorenzi; 4: Grotta di Florestano; 5: Riparo Mochi; 6: Riparo Blanc-Cardini; 7: Grotta del Caviglione; 8: Riparo Bombrini; 9: Barma Grande; 10: Grotta del Bausu da Ture; 11: Grotta del Principe; 12: site of the Ex-Casinò; 13: site of the Ex-Birreria (Drawing by Negrino, F.; modified from ref. *(106)*).

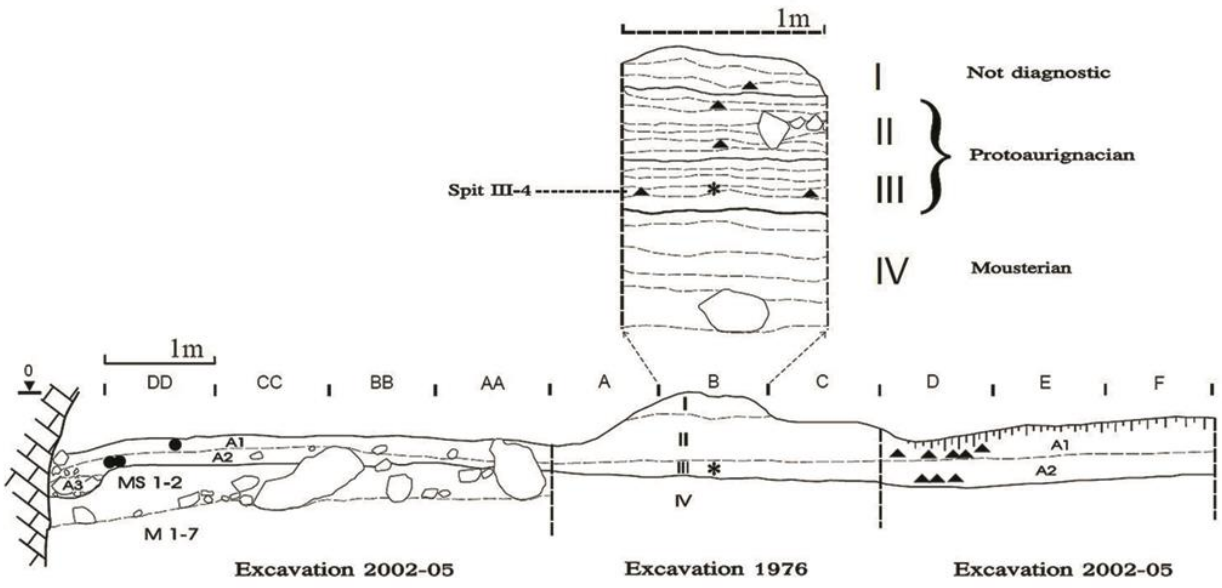

Fig. S3. Stratigraphic equence of Riparo Bombrini. The asterisk indicates the position of the human tooth (level III - spit 4); triangles and circles indicate respectively the location of dated bone and charcoal samples (drawing by Negrino, F.).

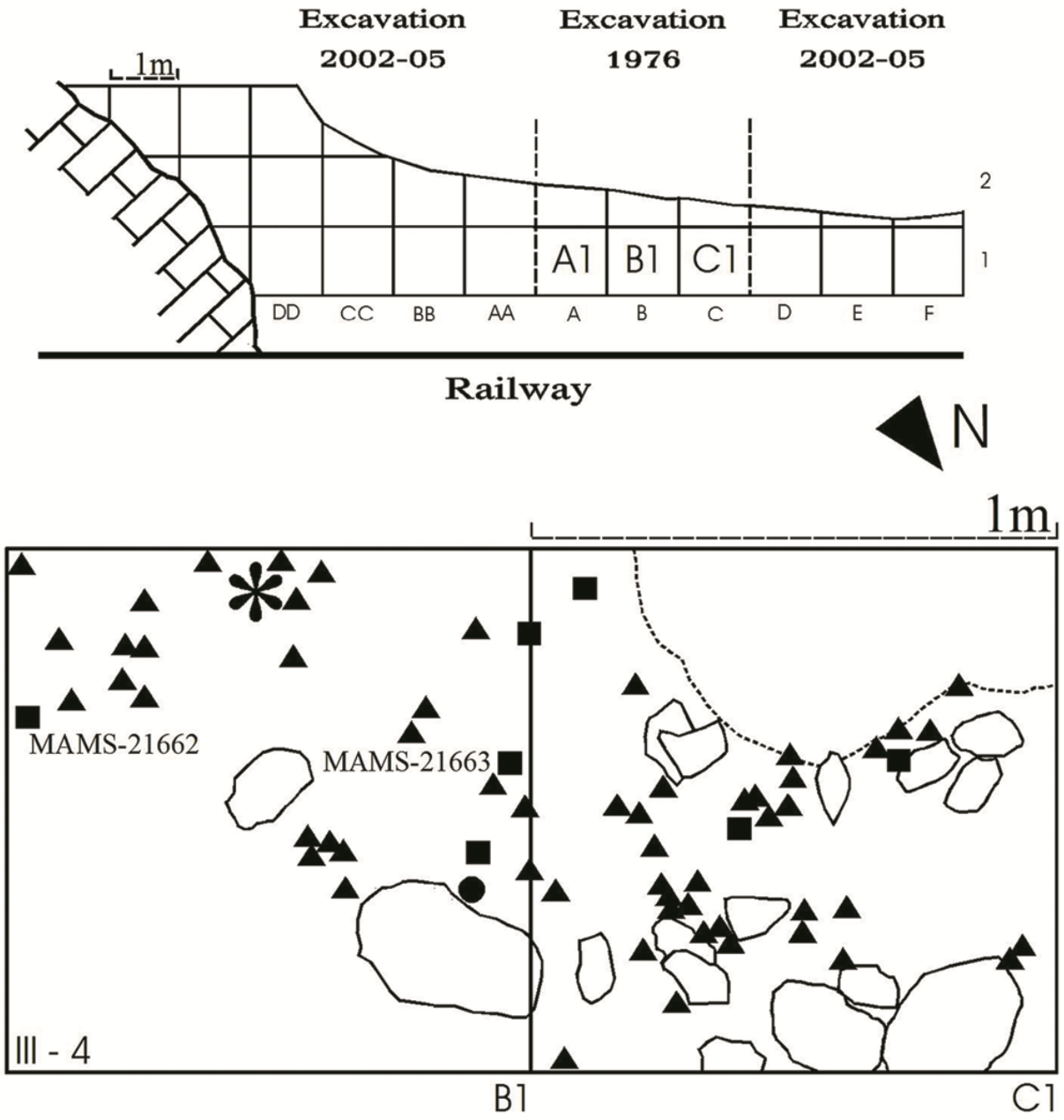

Fig. S4. Plan of the excavated area (above) and detail of squares B1-C1, Level III-spit 4, including mapped finds (below), **Riparo Bombrini**. Human tooth (asterisk), flint artefacts (triangles), red ochre (circle) and bones (squares), two of which dated (MAMS-21662 and MAMS-21663) (drawing by Negrino, F.; modified from ref. *(79)*).

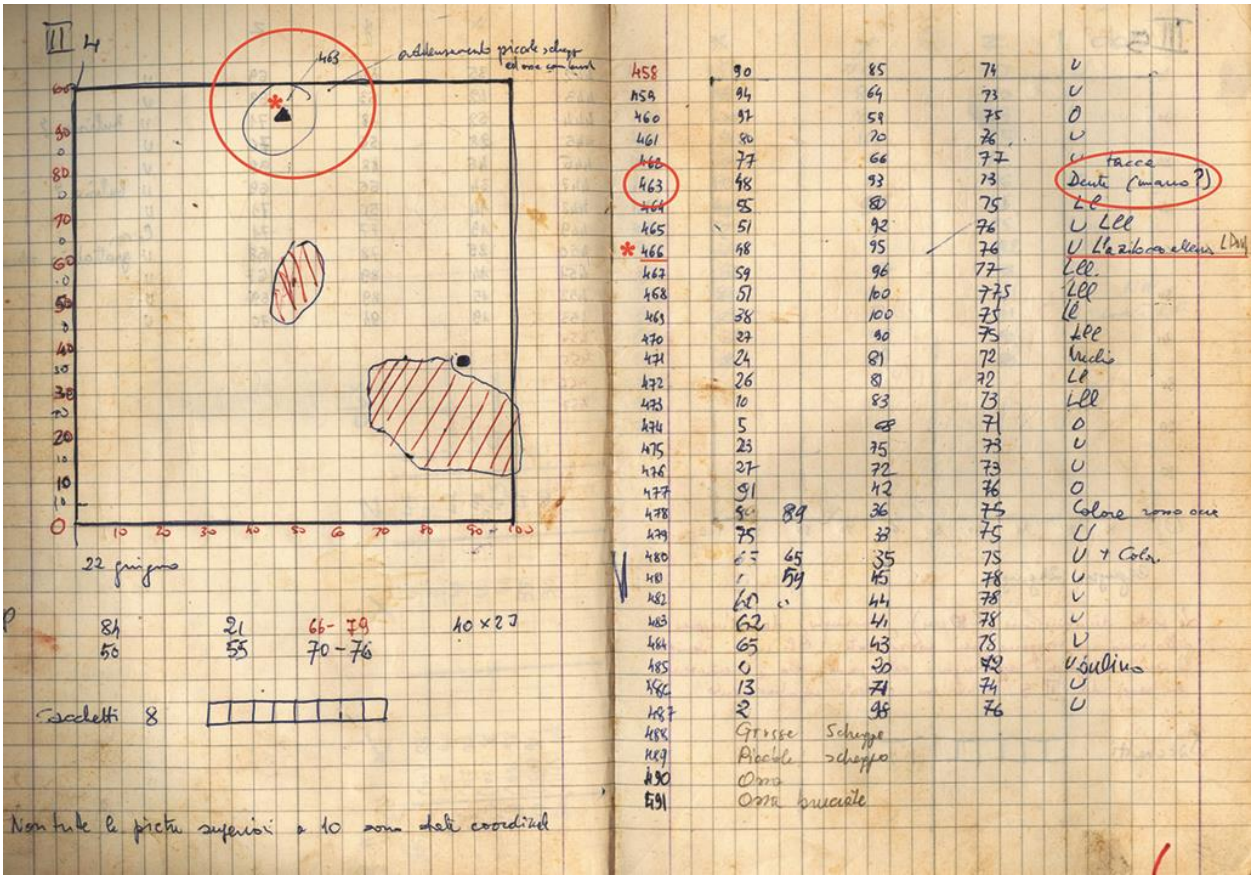

Fig. S5. The 1976 field journal by Giuseppe Vicino, illustrating square B1, Level III-spit 4, Riparo Bombrini. The triangle (n.463) indicates the human tooth, while the asterisk marks a Dufour bladelet (n.466).

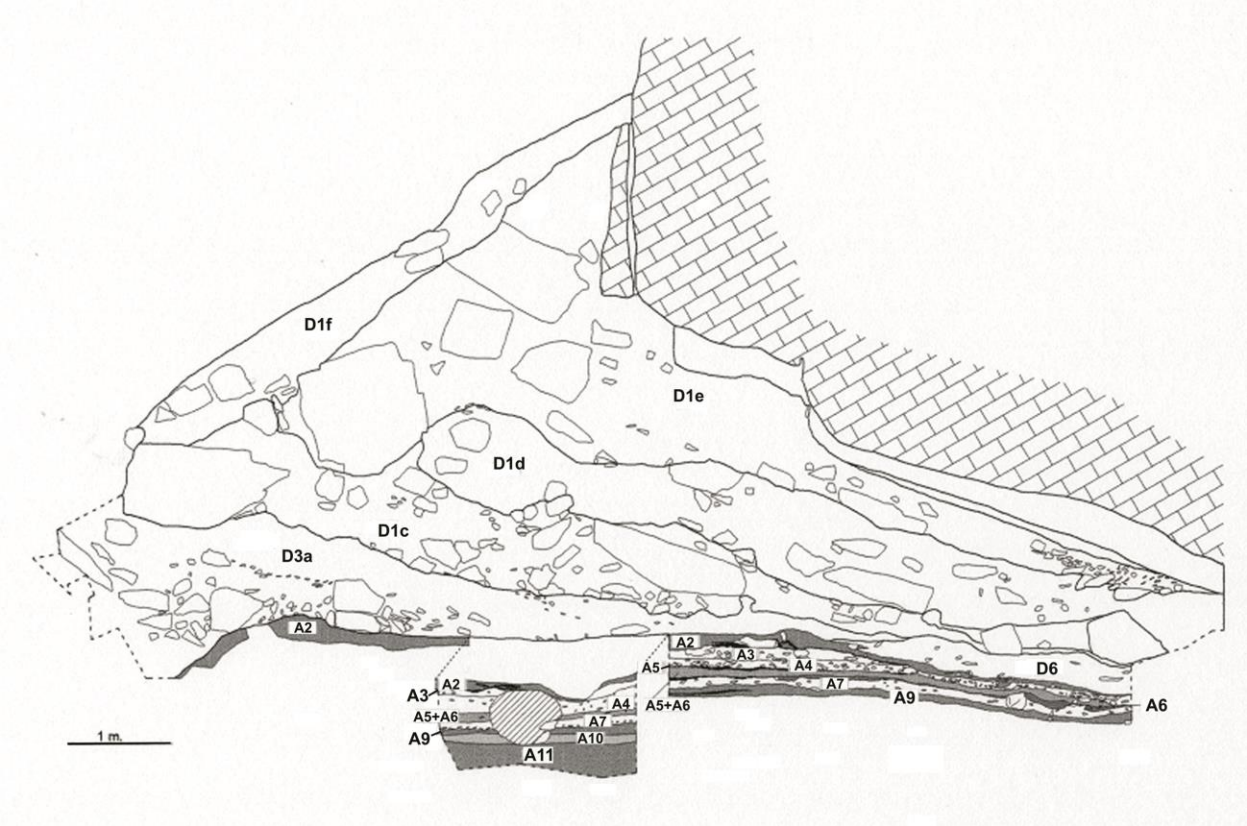

Fig. S6. Stratigraphic profile of Grotta di Fumane. Sketch section with evidence of late Mousterian (A11-A5), Uluzzian (A4-A3) and Protoaurignacian layers (A2), with variable content of archaeological remains (increasing from light gray to dark gray and black). (by M. Cremaschi, M. Peresani, redrawn by Muratori, S.).

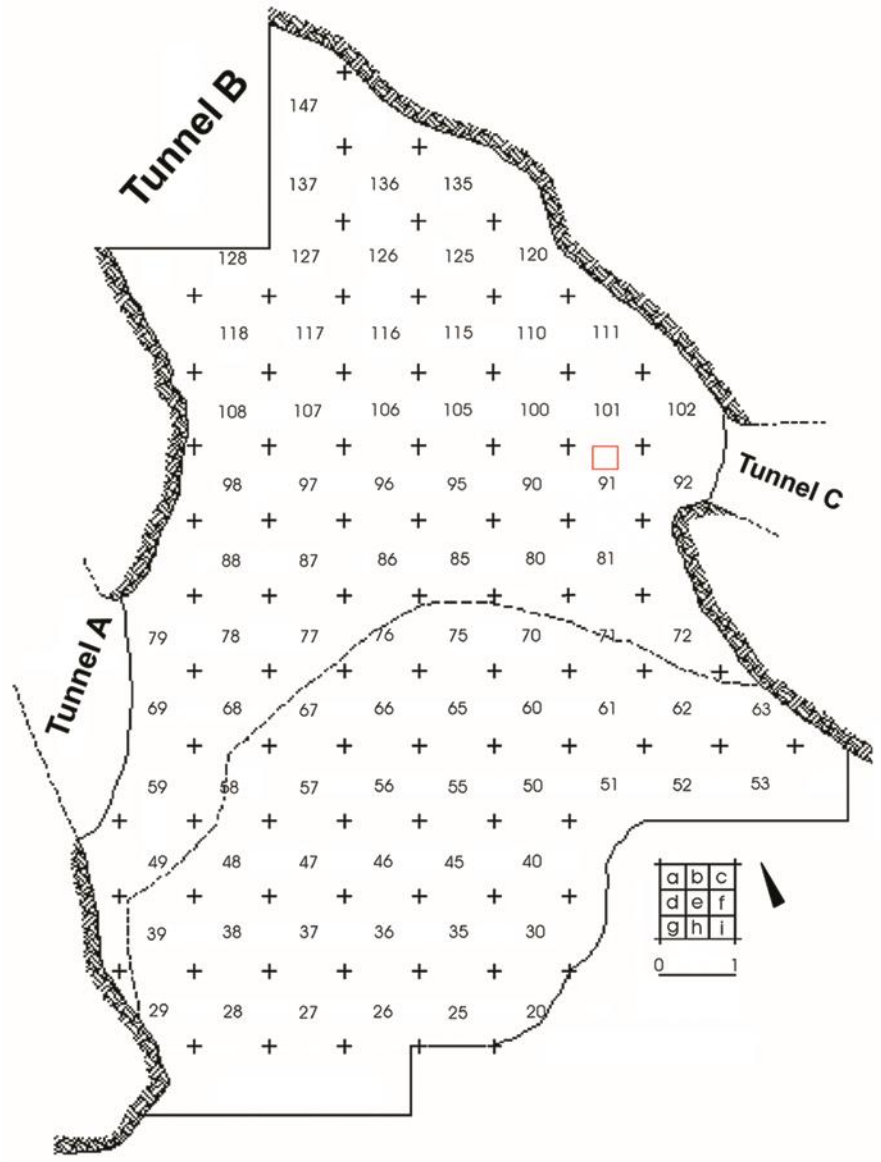

Fig. S7. Map of the excavated area of Grotta di Fumane. The red square marks the finding locus of the Fumane 2 specimen (square 91b).

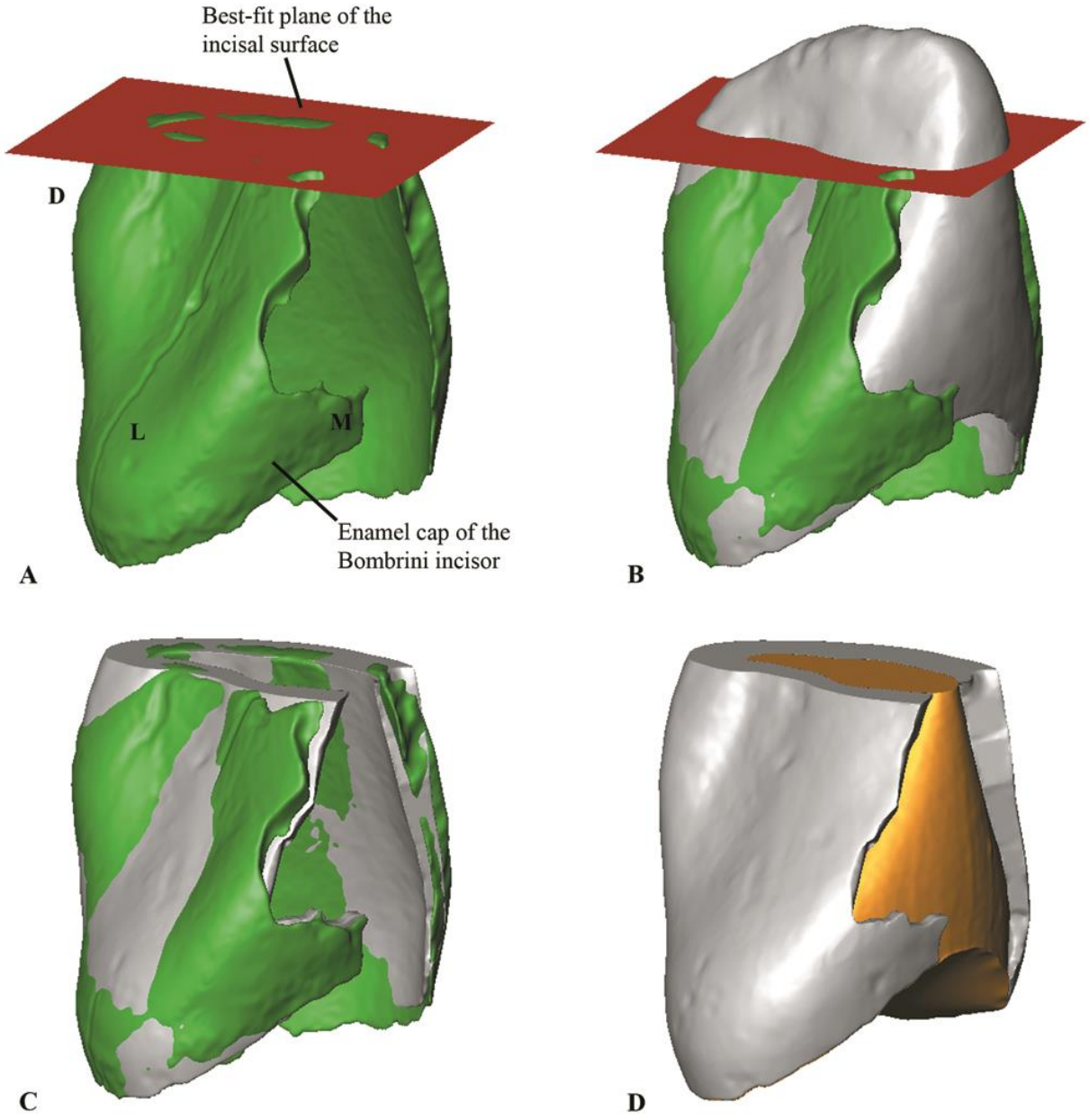

Fig. S8. Digital simulation of tooth wear and mesial damage in a modern human lower left lateral deciduous incisor (Ldi_2). A, A best-fit plane was interpolated on the incisal surface of the Bombrini Ldi_2**. B,** A modern human Ldi_2 (ID: SGVALD_T59) was superimposed to the Bombrini specimen using Iterative Closest Point algorithm. **C,** The portion of crown above the incisal plane and the portion of enamel in correspondence to the Bombrini's mesial damage were removed. **D,** The modern human specimen SGVALD_T59 virtually worn and damaged as the Bombrini Ldi_2. D, distal; L, lingual; M, mesial.

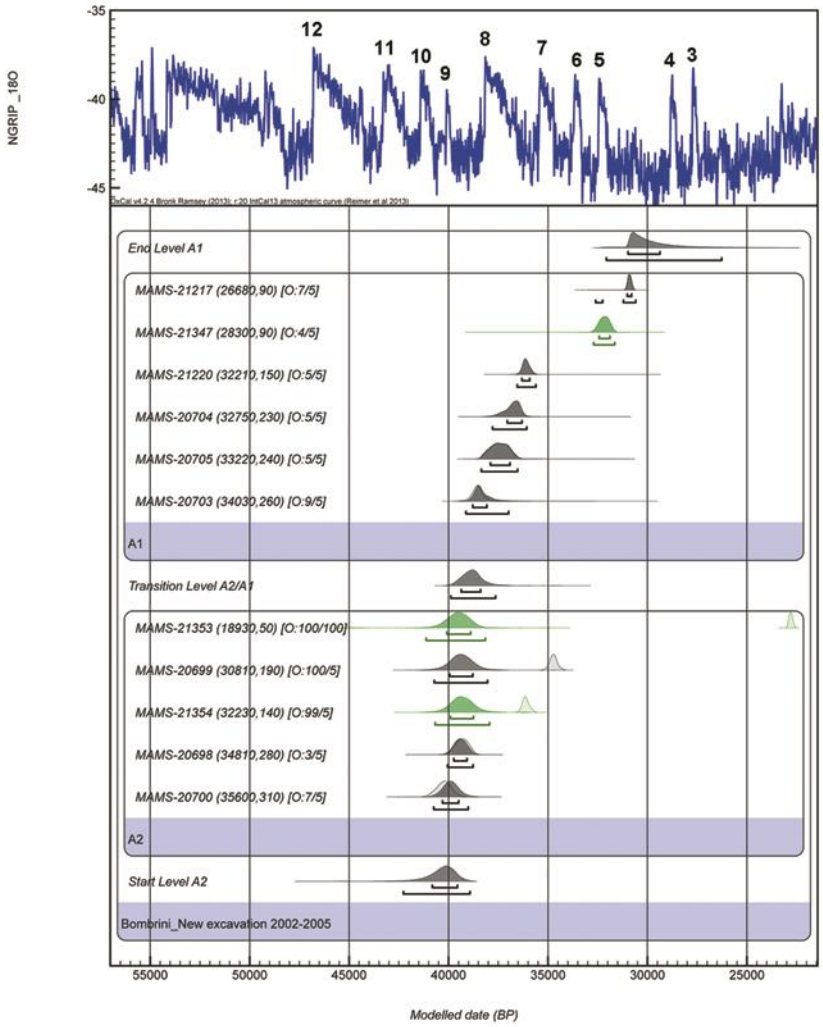

Fig. S9. Bayesian model of dates on organic remains from the 2002-2005 excavations at Riparo Bombrini. Radiocarbon dates are calibrated in IntCal13 *(24)*. Model and boundaries were computed by OxCal 4.2 *(29)*, including the performance of the General t-type Outlier Model *(29)*. Bone samples treated with ultrafiltration in grey; charcoal samples treated with ABOX in green. The results are linked with the (NGRIP) $\delta^{18}O$ climate record *(55, 56)*.

Table S1. Buccolingual (BL) diameters. Dental dimensions (in mm) of Bombrini and Fumane 2 standardized to Z-scores of the hominin samples[a-c] used in this study (m=mean; s=standard deviation; n=number of individuals).

	Bombrini (di_2)		Fumane 2 (di^2)	
	BL		BL	
	m ± s (n)	Z score	m ± s (n)	Z score
	4.6		5.5	
N	4.85±0.25 (15)[a]	-1.00	5.38±0.48 (9)[b]	0.25
UPHS	4.58±0.30 (18)[a]	0.07	5.12±0.29 (5)[b]	1.31
RHS	4.14±0.37 (62)[a]	1.24	4.7±0.4 (69)[c]	2.00

Based on [a]ref. *(107)*, [b]ref. *(108)* and [c]ref. *(109)*; N=Neandertals; UPHS=Upper Palaeolithic *Homo sapiens*; RHS=recent *Homo sapiens*

Table S2. Three-dimensional enamel thickness. Values of the components of 3D enamel thickness of Bombrini, Neandertals and recent *H. sapiens* (RHS) lower lateral deciduous incisors (di_2).

Taxon	Specimen ID	Side	Wear stage[a]	Enamel volume (mm^3)	Coronal dentine + pulp volume (mm^3)	EDJ[b] surface (mm^2)	3D AET[c] (mm)	3D RET[d] (scale-free)
Bombrini		L	4	10.87	31.01	37.53	0.29	9.22
Neandertals	Abri Suard	R	3	18.64	58.89	73.03	0.26	6.56
	Amud 7	L	1	21.14	50.93	69.59	0.30	8.20
	Kebara 1	L	2	20.25	52.24	71.89	0.28	7.54
	La Ferrassie 8	L	1	19.47	46.95	68.24	0.29	7.91
	Roc de Marsal 1	R	3	16.85	47.22	63.53	0.27	7.34
RHS	Guid T8	L	4	11.58	27.11	44.03	0.26	8.75
	Guid T20	R	4	10.66	30.82	48.70	0.22	6.98
	Guid T22	R	4	14.80	28.57	46.54	0.32	10.40
	Guid T38	L	3	11.00	26.50	46.07	0.24	8.01
	Guid T39	R	2	18.11	31.61	52.21	0.35	10.97
	Guid T41	L	3	15.85	32.98	49.23	0.32	10.04
	Guid T49B	R	4	11.90	27.92	45.97	0.26	8.53
	Guid TB65	L	3	11.77	26.47	46.09	0.26	8.57
	Roccap US26	R	2	16.40	27.75	46.02	0.36	11.77
	Sgvald T37	R	3	13.74	27.85	47.10	0.29	9.62
	Sgvald T53	L	3	16.98	35.06	55.88	0.30	9.28
	Sgvald T54	L	3	15.53	26.69	46.40	0.33	11.20
	Sgvald T59	R	2	15.80	27.47	45.57	0.35	11.49
	Vald_BC TB75	L	3	17.21	33.23	51.33	0.34	10.43
	Vald T64	L	3	14.96	28.18	46.45	0.32	10.58
	Vald TB43	R	3	13.81	29.23	48.62	0.28	9.22
	Vald TB72	L	3	15.07	25.29	43.33	0.35	11.85
	Vald TB124	L	3	17.27	29.46	50.95	0.34	10.97

[a]Based on ref. *(19)*; [b]EDJ=enamel-dentine junction; [c]AET=average enamel thickness index; [d]RET=relative enamel thickness index

Table S3. Three-dimensional enamel thickness of two recent *H. sapiens* specimens (Guid_T39 and Sgvald_T59). The specimens were digitally worn and damaged to simulate the condition of the Bombrini incisor.

Specimen ID	Simulation	Enamel volume (mm^3)	Coronal dentine + pulp volume (mm^3)	EDJ[a] surface (mm^2)	AET[b] (mm)	RET[c] (scale-free)
Guid_T39	Original	18.11	31.61	52.21	0.35	10.97
	Bombrini's wear stage	13.17	29.71	43.08	0.31	9.87
	Bombrini's wear stage and damage	10.86	29.71	36.11	0.30	9.71
Sgvald_T59	Original	15.80	27.47	45.57	0.35	11.49
	Bombrini's wear stage	12.87	26.73	40.92	0.31	10.52
	Bombrini's wear stage and damage	11.14	26.73	35.2	0.32	10.58

[a]EDJ=enamel-dentine junction; [b]AET=average enamel thickness index; [c]RET=relative enamel thickness index

Table S4. General characteristics of the three libraries generated.

Library ID	Extract used (μl)	USER treated	Total molecule count	Number of raw sequences	Number of aligned sequences	Sequences mapped [%]	Number of unique sequences	Average number of duplicates
A4678	5	-	3.78E+09	2,902,307	129,057	4.4	4,590	27.6
A4679	15	-	9.40E+09	3,204,305	196,103	6.0	9,722	19.7
L9358	10	+	1.66E+10	1,176,132	21,953	1.9	3,531	6.2

Table S5. Frequencies of C to T substitutions at terminal positions of the sequences

Library ID	All sequences		Sequences with 3’ C to T	Sequences with 5’ C to T
	5’ C to T [%] (95% CI)	3’ C to T [%] (95% CI)	5’ C to T [%] (95% CI)	3’ C to T [%] (95% CI)
A4678	16.4 (14.3-18.9)	14.2 (12.1-16.6)	34.3 (20.8-50.8)	30.8 (18.6-46.4)
A4679	17.2 (15.6-18.9)	17.4 (15.8-19.2)	25.0 (17.1-35.0)	29.3 (20.2-40.4)
L9358	5.9 (4.4-7.9)	16.3 (13.6-19.4)	4.3 (0.8-21.0)	11.1 (2.0-43.5)

C, cytosine; T, thymine

Table S6. AMS radiocarbon results of 16 samples from Riparo Bombrini from the 2002-2005 and 1976 excavations. For the bone samples we included the isotopic values, C:N ratios and the amount of collagen extracted (%Coll), which refer to the >30 kDa fraction. $\delta^{13}C$ values are reported relative to the vPDB standard and $\delta^{15}N$ values are reported relative to the AIR standard. The humanly modified bones are indicates by an * next to the MPI Lab Code.

New Excavations (2002-2005)													**Cal BP from**	**Cal BP to**	**Cal BP from**	**Cal BP to**
MPI Lab Nr.	**Square nr.**	**U.S.**	**Material**	**% Coll**	**$\delta^{13}C$**	**$\delta^{15}N$**	**%C**	**%N**	**C:N**	**AMS nr.**	**^{14}C Age**	**1σ Err**	**68.20%**		**95.40%**	
S-EVA 29022	D1-III/3	Level A1	Bone	1.2	-19.6	5.4	45.2	15.8	3.3	MAMS-20703	34,030	260	38,830	38,280	39,170	37,810
S-EVA 29026	D1-III/3 16 nº62	Level A1	Bone	0.7	-19.3	6.3	41.9	14.6	3.4	MAMS-20705	33,220	240	37,910	36,940	38,300	36,640
S-EVA 29023	D1-III/3 13 nº14	Level A1	Bone	1.3	-19.0	5.9	39.8	14.0	3.3	MAMS-20704	32,750	230	37,020	36,320	37,630	36,150
S-EVA 29021	D1-III/2 22 nº31	Level A1	Bone	1.1	-19.4	4.9	44.3	15.4	3.4	MAMS-21220	32,210	150	36,300	35,940	36,440	35,720
S-EVA 29194*	D1 III/3 76 20	Level A1	Bone	1.0	-19.3	4.2	36.7	12.3	3.5	MAMS-21217	26,680	90	31,000	30,800	31,080	30,700
S-EVA-29889	DD1 III 1 n.24	Level A1	Charcoal							MAMS-21347	28,300	90	32,430	31,890	32,650	31,690
S-EVA 29017*	D1-III/5 nº133	Level A2	Bone	1.4	-19.0	5.6	43.1	15.7	3.2	MAMS-20700	35,600	310	40,590	39,830	41,010	39,490
S-EVA 29015	D1-III/5 16	Level A2	Bone	1.7	-19.4	5.1	43.0	15.7	3.2	MAMS-20698	34,810	280	39,670	38,960	40,010	38,680
S-EVA 29016	D1-III/5 17	Level A2	Bone	0.8	-19.2	6.8	43.1	15.5	3.2	MAMS-20699	30,810	190	34,930	34,540	35,130	34,310
S-EVA-29895	DD1 III 3a n.99	Level A2	Charcoal							MAMS-21354	32,230	140	36,310	35,960	36,450	35,750
S-EVA-29894	DD1 III 3a n.97	Level A2	Charcoal							MAMS-21353	18,930	50	22,900	22,700	22,970	22,600
Vicino Excavation (1976)													**Cal BP from**	**Cal BP to**	**Cal BP from**	**Cal BP to**
MPI Lab Nr.	**Square nr.**	**U.S.**	**Material**	**% Coll**	**$\delta^{13}C$**	**$\delta^{15}N$**	**%C**	**%N**	**C:N**	**AMS nr.**	**^{14}C Age**	**1σ Err**	**68.20%**		**95.40%**	
S-EVA-30845	B1 I/3 N33	Level I	Bone	0.9	-19.6	7.8	34.7	12.8	3.2	MAMS-22272	29,660	250	34,030	33,610	34,290	33,360
S-EVA-30847	B1 II/3	Level II	Bone	0.7	-19.8	5.4	40.3	14.4	3.3	MAMS-22273	31,780	320	36,050	35,330	36,330	34,980
S-EVA-30849	B1 II/7	Level II	Bone	0.7	-19.3	4.6	26.7	9.7	3.2	MAMS-22274	29,950	260	34,250	33,800	34,550	33,630
S-EVA-29896	B1 474 III 4	Level III	Bone	1.4	-19.2	6.5	44.1	14.9	3.5	MAMS-21662	33,980	160	38,670	38,340	38,870	38,110
S-EVA-29897	B1 460 III 4	Level III	Bone	0.9	-19.4	5.9	29.4	10.0	3.4	MAMS-21663	32,920	140	37,190	36,560	37,600	36,410

Table S7. AMS radiocarbon dating of Riparo Bombrini Mousterian level IV, published in ref. *(4)*.

Square identification	Material	AMS nr.	^{14}C Age	1σ Err
Bomb6-M3 IV,AA1 8 122	Shell	OxA-19862	40,340	390
Bomb 3-M5 IV,BB1 11	Shell	OxA-19291	38,140	260
Bomb7-M3 IV,AA1 8	Shell	OxA-20361	36,770	210
Bomb8-M2 IV, AA1 7	Shell	OxA-19292	36,540	240

Table S8. AMS radiocarbon dating of Grotta di Fumane Protoaurignacian level A2, published in ref. *(10)*.

Square identification	Material	AMS nr.	^{14}C Age	1σ Err
A2,struc.18	Charcoal	OxA-19584	35,850	310
A2,sq.97b	Charcoal	OxA-17569	35,640	220
A2,sq.107i	Charcoal	OxA-19570	35,180	220
A2,struc.17	Charcoal	OxA-19412	34,940	280
A2,struc.16/lev B	Charcoal	OxA-19414	34,180	270

Table S9. Calibrated boundaries for Riparo Bombrini (2002-2005 and Vicino 1976 excavations) and for the Protoaurignacian layers at Grotta di Fumane. The calibration was computed by OxCal 4.2 *(29)* using the International Calibration Curve IntCal13 *(24)* for terrestrial samples. The Marine 13 *(24)* calibration curve was used for the shell samples from the Mousterian level IV at Riparo Bombrini.

2002-2005 excavations	**Modelled (BP)**			
Indices **Amodel 17.1** **Aoverall 18.1**	**from**	**to**	**from**	**to**
	68.20%		**95.40%**	
End level A1	30,980	29,360	32,060	26,260
Transition level A2/A1	39,370	38,380	39,890	37,630
Start level A2	40,820	39,550	42,280	38,920
Vicino excavation (1976)	**Modelled (BP)**			
Indices **Amodel 67.6** **Aoverall 70.5**	**from**	**to**	**from**	**to**
	68.20%		**95.40%**	
End level I (Upper Palaeolithic)	33,990	32,660	34,150	30,140
Transition level II (Protoaurignacian) / level I(Upper Palaeolithic)	34,190	33,710	34,510	33,470
Transition level III/II (Protoaurignacian)	36,790	35,640	37,310	35,140
Transition level IV(Mousterian) / level III (Protoaurignacian)	40,710	38,940	40,960	38,460
Start level IV (Mousterian)	44,840	43,160	47,690	42,180
Fumane	**from**	**to**	**from**	**to**
Indices **Amodel 67.6** **Aoverall 70.5**	**68.20%**		**95.40%**	
Layer A2-A1	39,640	38,500	40,050	37,910
Protoaurignacian	40,430	39,200	41,470	38,410
Layer A3-A2	41,110	39,920	42,590	39,610

References:

32. D. Panetta *et al.*, Analysis of image sharpness reproducibility on a novel engineered micro-CT scanner with variable geometry and embedded recalibration software. *Phys. Med.* **28**, 166-173 (2012).
33. L. A. Feldkamp, L. C. Davis, J. W. Kress, Practical cone-beam algorithm. *J. Opt. Soc. Am. A* **6**, 612–619 (1984).
34. P. S. Ungar *et al.*, Neandertal incisor beveling. *J. Hum. Evol.* **32**, 407–421 (1997).
35. P. J. Besl, N. D. McKay, A method for registration of 3D shapes. *PAMI* **14**, 239–256 (1992).
36. J. Dabney *et al.*, Complete mitochondrial genome sequence of a Middle Pleistocene cave bear reconstructed from ultrashort DNA fragments. *Proc. Natl. Acad. Sci. USA* **110**, 15758–15763 (2013).
37. A. W. Briggs *et al.*, Removal of deaminated cytosines and detection of in vivo methylation in ancient DNA. *Nucleic Acids Res.* **38**, e87 (2010).
38. M. Meyer *et al.*, A high-coverage genome sequence from an archaic Denisovan individual. *Science* **338**, 222–226 (2012).
39. M.-T. Gansauge, M. Meyer, Single-stranded DNA library preparation for the sequencing of ancient or damaged DNA. *Nature Protocols* **8**, 737–748 (2013).
40. M. Meyer, M. Kircher, Illumina sequencing library preparation for highly multiplexed target capture and sequencing. *Cold Spring Harb Protoc.* **2010** (6): pdb.prot5448 (2010).
41. M. Kircher, S. Sawyer, M. Meyer, Double indexing overcomes inaccuracies in multiplex sequencing on the Illumina platform. *Nucleic Acids Res.* **40**, e3 (2012).
42. J. Dabney, M. Meyer, Length and GC-biases during sequencing library amplification: A comparison of various polymerase-buffer systems with ancient and modern DNA sequencing libraries. *BioTechniques* **52**, 87–94 (2012).

43. T. Maricic, M. Whitten, S. Pääbo, Mutiplexed DNA Sequence Capture for Mitochondrial Genomes Using PCR Products. *PLoS ONE* **5**, e14004 (2010).
44. Q. Fu *et al.*, DNA analysis of an early modern human from Tianyuan Cave, China. *Proc. Natl. Acad. Sci. USA* **110**, 2223–2227 (2013).
45. M. Kircher, U. Stenzel, J. Kelso, Improved base calling for the Illumina Genome Analyzer using machine learning strategies. *Genome Biol.* **10**, R83 (2009).
46. M. Kircher, Analysis of high-throughput ancient DNA sequencing data. *Methods Mol. Biol.* **840**, 197–228 (2012).
47. H. Li, R. Durbin, Fast and accurate long-read alignment with Burrows-Wheeler transform. *Bioinformatics* **26**, 589–595 (2010).
48. S. Talamo, M. Richards, A comparison of bone pretreatment methods for AMS dating of samples >30, 000 BP. *Radiocarbon* **53**, 443-449 (2011).
49. R. Longin, New method of collagen extraction for radiocarbon dating. *Nature* **230**, 241-242 (1971).
50. T. A. Brown *et al.*, Improved Collagen Extraction by modified Longin method. *Radiocarbon* **30**, 171-177 (1988).
51. F. Brock, C. B. Ramsey, T. Higham, Quality assurance of ultrafiltered bone dating. *Radiocarbon* **49**, 187–192 (2007).
52. S. H. Ambrose, Preparation and Characterization of Bone and Tooth Collagen for Isotopic Analysis. *J. Archaeol. Sci.* **17**, 431–451 (1990).
53. G. J. V. Klinken, Bone Collagen Quality Indicators for Palaeodietary and Radiocarbon Measurements. *J. Archaeol. Sci.* 26, 687-695 (1999).
54. B. Kromer *et al.*, MAMS – A new AMS facility at the Curt-Engelhorn-Centre for Achaeometry, Mannheim, Germany. *Nucl. Instrum. Meth.* B **294**, 11-13 (2013).
55. K. K.Andersen *et al.*, The Greenland Ice Core Chronology 2005, 15–42 ka. Part 1: constructing the time scale. *Quater. Sci. Rev.* **25**, 3246-3257 (2006).

56. A. Svensson *et al.*, The Greenland Ice Core Chronology 2005, 15–42 ka. Part 2: comparison to other records. *Quater. Sci. Rev.* **25**, 3258-3267 (2006).
57. A. Del Lucchese *et al.*, in *Un siècle de construction du discours scientifique en Préhistoire* (26° Congrès Préhistorique de France, Avignon–Bonnieux 21-25, 2004), pp. 177-184.
58. M. Mussi, J. Cinq-Mars, P. Bolduc, Echoes from the mammoth steppe: the case of the Balzi Rossi. *Anal. Praehist. Leid* **31**, 105-124 (1999).
59. G. Vicino, Incisioni rupestri paleolitiche ai Balzi Rossi. *Riv. Ing. Int.* **26**, 51-56 (1971).
60. G. Vicino, Incisioni rupestri paleolitiche ai Balzi Rossi. *Riv. St. Lig.* **38**, 5-26 (1972).
61. G. Vicino, M. Mussi, Arte parietale ai Balzi Rossi: la Grotticella Blanc-Cardini (Ventimiglia, IM). *Origini* **23**, 21-38 (2011).
62. M.A. de Lumley, L'os iliaque anténéanderthalien de la grotte du Prince (Grimaldi, Ligurie italienne). *Bull. Mus. Anthropol. Préhist. Monaco* **18**, 89-112 (1972).
63. G. Vicino, Gli scavi preistorici nell'area dell'ex Casinò dei Balzi Rossi (Nota preliminare). *Riv. Ing. Int.* **27**, 77-97 (1972).
64. G. Vicino, La spiaggia tirreniana dei Balzi Rossi nei recenti scavi della zona dell'ex-casinò. *Atti della XVI Riunione Scientifica, Istituto Italiano di Preistoria e Protostoria, Firenze*, 75-95 (1974).
65. M. Cremaschi *et al.*, Ventimiglia (Imperia). Località Balzi Rossi. Nuovi dati sulla successione stratigrafica del ciclo interglaciale-glaciale-postglaciale. Scavi 1990. *Bollettino di Archeologia* **8**, 47-50 (1991).
66. A. Bietti, F. Negrino, in *New Approaches to the Study of Early Upper Palaeolithic "Transitional" Industries in Western Eurasia. Transitions Great and Small*, J. Riel-Salvatore, G. A. Clark, Eds. (B.A.R., Oxford, 2007), pp. 41-60.
67. A. Bietti, F. Negrino, L'Aurignacien et le Gravettien du Riparo Mochi, l'Aurignacien du Riparo Bombrini: comparaisons et nouvelles perspectives. *Arch. Inst. Pal. Hum.* **39**, 133-140 (2008).
68. A. Bietti, A. Del Lucchese, F. Negrino, Nuovi studi e ricerche al Riparo Mochi (Balzi Rossi, Ventimiglia, Imperia). *Paleo-express* **7**, 4-6 (2001).
69. A. Bietti *et al.*, in *Archeologia in Liguria, Nuova Serie, I, 2004-2005*, A. Del Lucchese, L. Gambaro, Eds. (Soprintendenza per i Beni Archeologici della Liguria, Genova, 2008), pp. 237-238.

70. K. Douka *et al.*, A new chronostratigraphic framework for the Upper Palaeolithic of Riparo Mochi (Italy). *J. Hum. Evol.* **62**, 286-299 (2012).
71. A. Tagliacozzo *et al.*, Archaeozoological evidence of subsistence strategies during the Gravettian at Riparo Mochi (Balzi Rossi, Ventimiglia, Imperia - Italy). *Quat. Int.* **252**, 142-154 (2012).
72. C. Tozzi, F. Negrino, Nouvelles données sur les cultures moustériennes des grottes de Grimaldi. *Arch. Inst. Pal. Hum.* **39**, 101-107 (2008).
73. V. Formicola, P. B. Pettitt, A. Del Lucchese, A Direct AMS Radiocarbon Date on the Barma Grande 6 Upper Paleolithic Skeleton. *Curr. Anthropol.* **45**, 114-118 (2004).
74. V. Formicola, B. Holt, I resti umani del Paleolitico superiore della Liguria Occidentale: Una sintesi sui risultati degli studi recenti. *Bull. Mus. Anthropol. Préhist. Monaco*, **suppl. 1**, 96-102 (2008).
75. B. Holt, V. Formicola, Hunters of the Ice Age: The biology of Upper Paleolithic people. *Am. J. Phys. Anthropol.* **S47**, 70-99 (2008).
76. É. Rivière, De l'antiquité de l'homme dans les Alpes-Maritimes (Paris, 1887).
77. L. Cardini, Recenti scavi dell'Istituto Italiano di Paleontologia Umana alla Barma Grande di Grimaldi. *Arch. Antr. Etn.* **68**, 385-389 (1938).
78. G. Vicino, Lo scavo paleolitico al Riparo Bombrini (Balzi Rossi di Grimaldi, Ventimiglia). *Riv. Ing. Int.* **39**, 1-10 (1984).
79. V. Formicola, Un incisivo umano deciduo dal deposito aurignaziano del Riparo Bombrini ai Balzi Rossi. *Riv. Ing. Int.* **39**, 11-12 (1984).
80. D. Arobba, R. Caramiello, Analisi paleobotanica sui sedimenti del riparo Bombrini (Balzi Rossi, Ventimiglia). *Bull. Mus. Anthropol. Préhist. Monaco* **49**, 41-48 (2009).
81. S. Bertola *et al.*, La diffusione del primo Aurignaziano a sud dell'Arco alpino. *Preistoria Alpina* **47**, 17-30 (2013).
82. A. Del Lucchese *et al.*, Riparo Bombrini, Balzi Rossi (Ventimiglia, Imperia). Notizie preliminari degli scavi 2002-2004. *Ligures* **2**, 287-289 (2004).
83. F. Negrino, Riparo Bombrini, Balzi Rossi (Ventimiglia, IM): la campagna 2005. *Ligures* **3**, 194-196 (2005).
84. F. Negrino, C. Tozzi, Il Paleolitico in Liguria. *Bull. Mus. Anthropol. Préhist. Monaco* **suppl. 1**, 21-28 (2008).

85. J. Riel-Salvatore *et al.*, A spatial analysis of the Late Mousterian levels of Riparo Bombrini (Balzi Rossi, Italy), *Can. J. Archaeol.* **37**, 70-92 (2013).
86. S. Bertola, Approccio micropaleontologico discriminante per riconoscere la provenienza alpina o appenninica delle selci della scaglia rossa (Italia centro-settentrionale). *Bull. Mus. Anthropol. Préhist. Monaco* **52**, 17-27 (2012).
87. F. Negrino, E. Starnini, in *Les Matières Premières Lithiques en Préhistoire* (Actes de la Table ronde internationale, Aurillac, France, 2003), pp. 235-243.
88. M. Martini *et al.*, Thermoluminescence (TL) dating of burnt flints: problems, perspectives and some example of application. *J. Cult. Herit.* **2**, 179-190 (2001).
89. M. Peresani *et al.*, Age of the final Middle Palaeolithic and Uluzzian levels at Fumane Cave, Northern Italy, using 14C, ESR, 234U/230Th and thermoluminescence methods. *J. Arch. Sci.* **35**, 2986–2996 (2008).
90. P. F. Cassoli, A. Tagliacozzo, Considerazioni paleontologiche, paleoeconomiche e archeozoologiche sui macromammiferi e gli uccelli dei livelli del Pleistocene superiore del Riparo di Fumane (VR) (Scavi 1988-91). *Boll. Mus. Civ. Stor. Nat. Verona* **18,** 349-445 (1991).
91. M. Peresani, A new cultural frontier for the last Neanderthals: the Uluzzian in Northern Italy. *Curr. Anthropol.* **49**, 725–731 (2008).
92. C.A. Jéquier, M. Romandini, M. Peresani, Les retouchoirs en matières dures animales: une comparaison entre Moustérien final et Uluzzien. *Comptes Rendus Palevol* **11**, 283-292 (2012).
93. M. Peresani, Fifty thousand years of flint knapping and tool shaping across the Mousterian and Uluzzian sequence of Fumane cave. *Quat. Int.* **247**, 125-150 (2012).
94. M. Peresani *et al.*, Fire-places, frequentations and the environmental setting of the final Mousterian at Grotta di Fumane: a report from the 2006-2008 research. *Quartär.* **58**, 131-151 (2011).
95. M. Peresani *et al.*, Late Neandertals and the intentional removal of feathers as evidenced from bird bone taphonomy at Fumane cave 44ky BP, Italy. *Proc. Natl. Acad. Sci. U S A* **108**, 3888-3893 (2011).

96. M. Peresani, L. Centi, E. Di Taranto, Blades, bladelets and flakes: a case of variability in tool design at the onset of the Middle – Upper Palaeolithic transition in Italy. *Comptes Rendus Palevol* **12**, 211-221 (+corrigendum) (2013).
97. M. Romandini *et al.*, The ungulate assemblage from layer A9 at Grotta di Fumane, Italy: a zooarchaeological contribution to the reconstruction of Neanderthal ecology. *Quat. Int.* **337**, 11–27 (2014).
98. A. Broglio, L'estinzione dell'Uomo di Neandertal e la comparsa dell'Uomo moderno in Europa. Le evidenze della Grotta di Fumane nei Monti Lessini. *Atti Istituto Veneto SS.LL.AA* **45**, 1–44 (1997).
99. A. Broglio, F. Gurioli, in *La spiritualité. Etudes et Recherches Archéologiques 106*, M. Otte, Ed. (Université de Liège, Liège, 2004), pp. 97–102.
100. C. Peretto *et al*., Living-Floors and Structures From the Lower Palaeolithic to the Bronze Age. *Coll. Anthrop.* **28**, 63-88 (2004).
101. A. Broglio *et al.*, in *Production lamellaires attribuèes à l'Aurignacien*, F. Le Brun-Ricalens, Ed. (Luxembourg, Musée National d'Histoire et d'Art, 2005), pp. 415–436.
102. A. Broglio *et al.*, in *Kostenki and the early Upper Paleolithic of Eurasia: General trends, local developments*, S. A. Vasil'ev *et al.*, Eds. (Nestor-Historia Saint Petersburg, 2006), pp. 263–268.
103. A. Broglio *et al*., L'art aurignacien dans la décoration de la Grotte de Fumane. *L'Anthropologie* **113**, 753–761 (2009).
104. D.H. Ubelaker, *Human Skeletal Remains. Excavations, Analysis, Interpretation* (Aldine, Chicago, 1978).
105. S. J. AlQahtani, M.P. Hector, H.M. Liversidge, The London atlas of human tooth development and eruption. *Am. J. Phys. Anthropol.* **142**, 481–490 (2010).
106. P. Graziosi, I Balzi Rossi. Itinerari Liguri 2 (Istituto Internazionale di Studi Liguri, Bordighera, 1976).
107. I. Crevecoeur *et al.*, The Spy VI child: a newly discovered Neandertal infant. *J. Hum. Evol.* **59**, 641–656 (2010).
108. E. Trinkaus, V. A. Ranov, S. Lauklin, Middle paleolithic human deciduous incisor from Khudji, Tajikistan. *J. Hum. Evol.* **38**, 575-583 (2000).

109. T. K. III. Black, Sexual dimorphism in the tooth-crown diameters of the deciduous teeth. *Am. J. Phys. Anthrop*. **48**, 77–82 (1978).